

Inelastic transport in molecular spin valves

N. Jean and S. Sanvito*

School of Physics, Trinity College, Dublin 2, IRELAND

(Dated: November 16, 2017)

We present a study of the effects of inelastic scattering on the transport properties of various nanoscale devices, namely H_2 molecules sandwiched between Pt contacts, and a spin-valve made by an organic molecule attached to model half-metal ferromagnetic current/voltage probes. In both cases we use a tight-binding Su-Schrieffer-Heeger Hamiltonian and the inelastic effects are treated with a multi-channel method, including Pauli exclusion principle. In the case of the H_2 molecule, we find that inelastic backscattering is responsible for the drop of the differential conductance at biases larger than the excitation energy of the lower of the molecular phonon modes. In the case of the spin-valve, we investigate the different spin-currents and the magnetoresistance as a function of the position of the Fermi level with respect to the spin-polarized band edges. In general inelastic scattering reduces the spin-polarization of the current and consequently the magnetoresistance.

PACS numbers:

I. INTRODUCTION

Recent years have witnessed an increasing interest for spintronics devices and for their possible application as novel elements in microelectronics industry [1, 2, 3]. Read-heads based on the giant magnetoresistance (GMR) effect [4, 5] have already revolutionized the hard-drives market and other magnetic devices such as magnetic random access memory (MRAM) are expected to have a similar or even bigger impact. These devices exploit both the magnetic and the electronic properties of conducting materials.

In the typical spin-valve geometry a non-magnetic spacer is sandwiched between two magnetic contacts. These provide a source of spin-polarized electrons and the device practically behaves as a polarizer/analyzer spin filter, with the magnetization vector establishing the polarization axis. Typically the resistance of the device is higher when the magnetization vectors of the contacts are aligned antiparallel to each other, and drops when the alignment is parallel. The non-magnetic spacer controls the total resistance of the device and the overall transport regime (diffusive, ballistic, tunneling, etc.), while the quality and nature of the interfaces can further affect the spin polarization.

Many suggestions for possible non-magnetic spacers have been recently proposed [6]. Among the most intriguing there is the possibility of using organic molecules [7]. These offer low fabrication costs and high manufacturability typical of molecular electronics [8, 9] and the advantage of long spin-relaxation times. Several prototypes for molecular spin-valves have been already fabricated and GMR in excess of 10% have been reported for spacers such as π -conjugated molecules [10, 11] and in organic tunneling junctions [12].

Electron conduction through these systems is always

explained in terms of elastic transport [7, 13, 14] and inelastic effects are often neglected. This may be a quite drastic simplification in particular in the case of thick organic spacers, for which the transmission due to direct tunneling becomes negligible. Inelastic scattering not only does open new transport channels but also affects the transmission of the elastic ones by introducing competition for the same final states due to the Pauli exclusion principle [15, 16]. These effects can change drastically the conducting properties of the devices and affect the GMR of spin-valves. Recent experimental and theoretical works have already shown the importance of the inelastic scattering in different non-magnetic molecular devices [17, 18, 19, 20, 21, 22, 23, 24].

In this work we investigate the effects of inelastic scattering on the transport properties of model spin-valves. First, we briefly introduce our method for calculating the I - V characteristics of a typical two probe device in presence of electron-phonon coupling. This is based on a combination of scattering theory in a Green's function framework [25, 26] and a self-consistent evaluation of the non-equilibrium electron distribution [16]. Then we show a typical calculation by investigating the transport properties of the H_2 molecule sandwiched between two platinum leads. Finally we consider the case of organic spin-valves obtained by sandwiching a mono-atomic chain, resembling the properties of a $(CH)_n$ molecule, between half-metallic leads. For this system we consider a model $M_{\beta'}$ half metal (according to the classification of Coey and Sanvito [27]), which resembles the electronic structure of magnetite.

II. COMPUTATIONAL METHOD

A. Problem set-up

The system under investigation is schematically represented in figure 1. It consists of two semi-infinite current/voltage probes formed from mono-atomic chains

*Electronic address: sanvitos@tcd.ie

and sandwiching a scattering region (the molecule). Electron-phonon interaction is present only in the scattering region while the leads act as an ideal phonon sink. The scattering region is composed by one or more atoms



FIG. 1: Schematic representation of a system composed of two semi-infinite current/voltage leads and a scattering region, where inelastic scattering can occur. An electron with k -vector k approaching the scattering region from the left is transmitted to the right with k -vector k' . In this 1D case if $k \neq k'$ the energy is not conserved.

connected to the leads both via electron and phonon-assisted hopping.

The Hamiltonian H describing such a system can be divided in five parts

$$H = H_L + V_{ML} + H_M + V_{MR} + H_R. \quad (1)$$

H_L (H_R) describes the left-hand side (right-hand side) lead, H_M describes the molecule and V_{ML} (V_{MR}) the interaction between the left (right) lead and the molecule. For the leads we consider a tight-binding model expanded over a s -like orthogonal basis set $|i\rangle$, where i labels the atomic position. Although there is no conceptual complication in considering a multi-orbital tight-binding model here we use only one orbital per atomic site in order to keep the computational overheads to a minimum. This choice is motivated by the severe scaling of our computational method [16] with the number of phonons. Thus H_L and H_R read

$$H_L = \epsilon_L \sum_{i=-\infty}^0 c_i^\dagger c_i + \beta_L \sum_{i=-\infty}^{-1} (c_i^\dagger c_{i+1} + c.c.), \quad (2)$$

$$H_R = \epsilon_R \sum_{i=N+1}^{+\infty} c_i^\dagger c_i + \beta_R \sum_{i=N+1}^{+\infty} (c_i^\dagger c_{i+1} + c.c.). \quad (3)$$

In the expressions above c_i and c_i^\dagger are the annihilation and creation operators for electrons at the site i , β_α ($\alpha = R, L$) is the hopping parameter in the leads and ϵ_α is the lead on-site energy. This already include the rigid shift given by an external voltage V applied to the system, that is $\epsilon_L = \epsilon_L^0 + \frac{V}{2}$ and $\epsilon_R = \epsilon_R^0 - \frac{V}{2}$, with $\epsilon_{L/R}^0$ the on-site energy for $V = 0$. Note that we implicitly assume that the leads are good metals presenting local charge neutrality [28]. The leads extend from $-\infty$ to $i = 0$ to the left and from $N + 1$ to $+\infty$ to the right, with the molecule comprising N sites ($i = 1, N$).

In our model system the electron-phonon interaction is present only in the molecule and at the interface of this with the leads. We use for the description of such a scattering region the Su-Schrieffer-Heeger (SSH) Hamiltonian [29, 30, 31] in its second quantization form, considering

only longitudinal phonon modes [24]. Thus H_M reads

$$H_M = \epsilon_M \sum_{i=1}^N b_i^\dagger b_i + \sum_{i \neq j} t_{ij} (b_i^\dagger b_j + b_j^\dagger b_i) + \sum_k \hbar \omega_k a_k^\dagger a_k + \sum_k \sum_{i \neq j} \gamma_{ij}^k (a_k^\dagger + a_k) (b_i^\dagger b_j + b_j^\dagger b_i). \quad (4)$$

Such a SSH-like Hamiltonian describes linear electron-phonon coupling. It has a purely electronic part written in a tight-binding form with annihilation and creation operators b_i and b_i^\dagger , hopping parameter t_{ij} and on-site energy ϵ_M . These tight-binding parameters refer to the static system (without phonons). In addition there is an electron-phonon interaction part $\sum_k \sum_{i \neq j} \gamma_{ij}^k (a_k^\dagger + a_k) (b_i^\dagger b_j + b_j^\dagger b_i)$, which describes phonon absorption/emission. This is linear in the phonon annihilation and creation operators a_k and a_k^\dagger with the coupling strength given by γ_{ij}^k . Finally it comprises the purely phononic energy $\sum_k \hbar \omega_k a_k^\dagger a_k$ with ω_k the phonon frequency for the k -mode. The frequencies ω_k are calculated using a classical “springs and balls” model for the scattering region [32], i.e. by diagonalizing the dynamical matrix obtained with the appropriate boundary conditions (see figure 2).

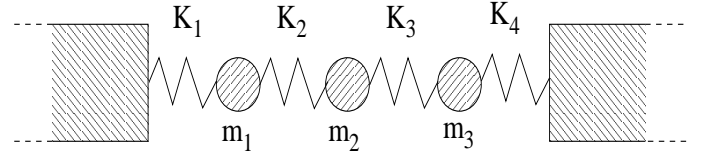


FIG. 2: Classical “springs and balls” model used to calculate the phonon modes. The leads act as hard walls constraining the oscillation to the middle atomic chain. m_j are the masses of the atoms in the scattering region and K_j are the spring constants.

The parameter γ_{ij}^k depends on both the energy of the k -mode, $\hbar \omega_k$, and the vibrational properties of the atomic sites i and j . It can be written as

$$\gamma_{ij}^k = \alpha_{ij} \left\{ \frac{e_k^i}{\sqrt{m_i}} - \frac{e_k^j}{\sqrt{m_j}} \right\} \sqrt{\frac{\hbar}{2\omega_k}} \quad (5)$$

where e_k^i is the displacement vector of the i -th atom associated to the k -mode, m_i (m_j) is the mass of the i -th (j -th) atom and α_{ij} is the coefficient of the linear expansion of the hopping parameter over the atomic displacement

$$t(q_i - q_j) = t_{ij} + \alpha_{ij}(q_i - q_j). \quad (6)$$

In the previous equation t_{ij} is the first term of the expansion and stands for the hopping parameter of the static system at the equilibrium distance, while q_i and q_j are the displacements from the equilibrium positions of the atoms i and j due to the lattice vibrations.

The Hamiltonian coupling the molecule to the leads is again of a SSH form

$$V_{\text{ML}} = \left[w^0 + \sum_k \Gamma^k (a_k^\dagger + a_k) \right] (c_0^\dagger b_1 + b_1^\dagger c_0), \quad (7)$$

with an analogous expression for V_{MR} . The purely elastic part is described by the hopping parameter w^0 while the inelastic part is characterized by the electron phonon coupling Γ^k

$$\Gamma^k = \alpha_1 \frac{e_k^1}{\sqrt{m_1}} \sqrt{\frac{\hbar}{2\omega_k}}. \quad (8)$$

The equation (8) is obtained from the (5) by imposing static boundary conditions to the leads ($q_i = 0$ for i belonging to the leads).

B. Inelastic scattering as an effective elastic problem

We tackle the problem of transport in presence of electron-phonon interaction by using the method proposed first by Bonča and Trugman [33, 34]. This approach consists in mapping a general many-body transport problem onto a fictitious one-body problem, where only elastic scattering is present. The method, in contrast to other perturbative approaches [35], is in principle exact. i.e. it does not introduce any approximation in calculating the inelastic contributions to the current. The drawback is cast in the dimension of the Hilbert space needed for defining the fictitious one-body system, which grows rapidly with the number of phonon states considered. In this section we will restrain our attention to mono-atomic single-channel leads, but the same procedure can be easily extended to the multichannel case [36]

The main idea behind this approach is that the energy is globally conserved during the scattering process. In fact, although an electron leaving the left-hand side lead with energy E and emitting a phonon is absorbed by the right-hand side lead with a different energy E' , the energy of the system electron plus phonon is conserved ($E - E'$ is the phonon energy). This suggests the possibility of constructing an associated multi-channel scattering problem [37], using asymptotic states that include both electronic and phononic degrees of freedom, all having the same total energy. In this way the scattering problem is formally elastic and can be solved by standard scattering theory [15, 25]. However, when extracting the electron current, one should be able to map this fictitious problem back to the original many-body one.

We then define states $|k; n_\alpha, n_\beta, \dots\rangle$ where the electronic part $|k\rangle$ describes an asymptotic Bloch state k in the leads, and the phononic part $|n_\alpha, n_\beta, \dots\rangle$ is a Fock state associated to the various phonon modes α, β, \dots of the molecule. Here n_α is the occupation number of

the mode α . During a generic scattering event the total energy of such state $E = E_k + \hbar \sum_\alpha (n_\alpha \omega_\alpha)$ is conserved, despite the fact that the electronic energy E_k may not be. Therefore the scattering between the asymptotic states $|k; n_\alpha, n_\beta, \dots\rangle$ of this fictitious system is formally elastic. Note however that the Bloch states $|k\rangle$ asso-

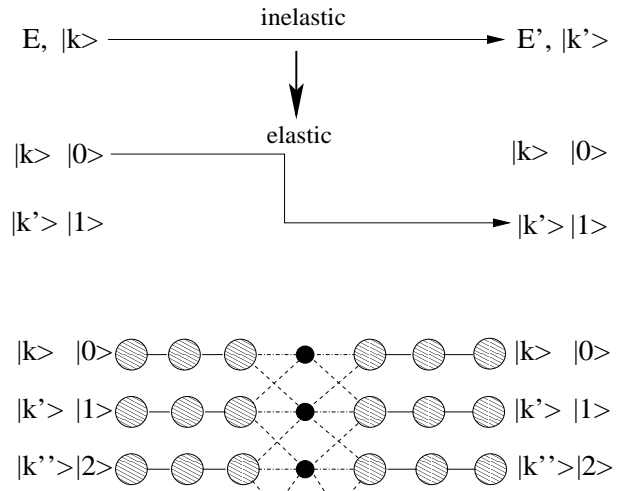


FIG. 3: Mapping procedure for a mono-atomic system with only one phonon mode. (a) During an inelastic process electrons change their energy from E to E' . In contrast in our fictitious system the scattering between states with different electronic energy ($|k, 0\rangle \rightarrow |k', 1\rangle$) is elastic, since the total energy (electron plus phonon) is conserved. (b) A mono-atomic chain sandwiching a molecule with vibrational degrees of freedom is mapped onto an equivalent system of disconnected atomic chains coupled through a scattering region.

ciated to the different asymptotic states $|k; n_\alpha, n_\beta, \dots\rangle$ in general have different energies, and must be calculated from the electronic secular equation at the energy $E_k = E - \hbar \sum_\alpha (n_\alpha \omega_\alpha)$. Importantly if the scattering is between states having identical phononic parts, then it is elastic not only for the fictitious system, but also for the actual many-body problem.

Therefore the mapping $|k\rangle \rightarrow |k; n_\alpha, n_\beta, \dots\rangle$ transforms an inelastic problem onto a fictitious multi-channel elastic one (see figure 3). For example within this approach a linear atomic chain sandwiching a vibrating molecule is formally equivalent to a collection of linear chains sandwiching an elastic scatterer, where the coupling between the chains is provided by the electron-phonon interaction only (see figure 3).

One can now construct a scattering theory for the asymptotic states $|k; n_\alpha, n_\beta, \dots\rangle$ by using one of the several methods available for elastic transport [26]. In this case however there are two additional features. First a new expression for the current, including Pauli exclusion principle, should be derived. In fact different incoming asymptotic states corresponding to electronic states with different energy may compete for the same final Bloch state. Secondly the dimension of the Hilbert space is in principle infinite, since the occupation numbers entering

the states $|k; n_\alpha, n_\beta, \dots\rangle$ are unbound. In practice however only a finite number of phonon modes is usually sufficient to obtain converged results, that is when the scattering transmission coefficients do not vary with the number of phonon states. Most importantly the convergence can be carefully monitored by progressively enlarging the Hilbert space.

C. Scattering theory

In the fictitious system, where the asymptotic states are $|k; n_\alpha, n_\beta, \dots\rangle$, the scattering is formally only elastic. Therefore we can calculate the quantum mechanical scattering probabilities by using standard scattering theory. In this work we have used the Green's function approach introduced by Sanvito et al. [25]. The method consists in evaluating the total retarded Green's function for the entire system (leads plus scattering region), from which extracting the scattering matrix. Here we briefly summarize the method and highlight the main modifications needed when dealing with the fictitious system, instead of a purely electronic one. Furthermore we consider simple one-dimensional leads, supporting only one scattering channel at a given energy.

The starting point consists in writing the surface Green's function for the leads. These are in the form of a block diagonal matrix, which, in the case of the left-hand side lead, reads

$$G_L^0(E) = \begin{pmatrix} g_L^0(E) & 0 & \dots & \dots \\ 0 & g_L^\mu(E') & \dots & \dots \\ \dots & \dots & g_L^{\mu'}(E'') & \dots \\ \dots & \dots & \dots & \dots \end{pmatrix}.$$

An analogous expression is valid for the right-hand side lead surface Green's function $G_R^0(E)$. $g_L^\mu(E')$ is the left surface Green's function of the purely electronic system (no phonons) at the energy E' . In general it is a $N \times N$ matrix, with N the number of degrees of freedom (orbitals) describing the leads surface, but in this simple case it is only a c-number

$$g_L^\mu(E') = \frac{e^{ik}}{\beta_L}, \quad (9)$$

with k the adimensional k -vector solution of the secular equation for the simple chain

$$E' = \epsilon_L + 2\beta_L \cos(k). \quad (10)$$

μ is a collective index, which label the phononic state $\mu = \{n_\alpha, n_\beta, \dots\}$ and the energy E' is the electronic energy of the state $|k; n_\alpha, n_\beta, \dots\rangle$, i.e. $E' = E - \hbar \sum_\alpha (n_\alpha \omega_\alpha)$. Note that the block diagonal form of G_L^0 and G_R^0 is the result of the fact that different phonon states $|n_\alpha, n_\beta, \dots\rangle$ do not mix in the leads. Note also that the Green's functions G_L^0 and G_R^0 are in principle infinite matrices since the number of possible phonon states

is infinite. In practice states with very large occupation numbers are not accessible and a cutoff N_{ph} over the number of phonon states is used.

In contrast to what happens in the leads, different phononic states do interact inside the scattering region. The matrix representing such an interaction is a $(M \cdot N_{\text{ph}}) \times (M \cdot N_{\text{ph}})$ hermitian matrix, where M is the number of electronic degrees of freedom (orbitals) describing the molecule. However, it is important to note that in this simple scattering approach, where no self-consistent evaluation of the scattering potential is carried out, it is possible to eliminate the explicit dependence of the scattering region Hamiltonian over the internal electronic degrees of freedom. This is done by using the recursive decimation method [25], to yield an effective energy-dependent $2N_{\text{ph}} \times 2N_{\text{ph}}$ Hamiltonian $H_{\text{eff}}(E)$, coupling all the phononic states in the left-hand side lead with those of the right-hand side lead

$$H_{\text{eff}}(E) = \begin{pmatrix} H_L^*(E) & H_{LR}^*(E) \\ H_{RL}^*(E) & H_R^*(E) \end{pmatrix}. \quad (11)$$

The blocks H_L^* and H_R^* describe the interaction respectively within the last plane of the left-hand side and first plane of the right-hand side lead, while the off diagonal blocks describe the coupling between these planes.

Finally the total Green's function of the system leads plus molecule calculated at the two extremal planes of the leads ($i=0$ and $i=N+1$) can be obtained by simply solving Dyson's equation

$$G(E) = [G^0(E)^{-1} - H_{\text{eff}}(E)]^{-1} = \begin{pmatrix} G_L & G_{LR} \\ G_{RL} & G_R \end{pmatrix}, \quad (12)$$

where $G^0(E)$ is written as

$$G^0(E) = \begin{pmatrix} G_L^0(E) & 0 \\ 0 & G_R^0(E) \end{pmatrix}. \quad (13)$$

The total Green's function G contains all the information about the scattering amplitudes. These can be explicitly extracted by using the Fisher and Lee relation [38] or in more general terms by projecting G over a general scattering wave-function [25, 26]. For our single-mode leads these simply read

$$t_{\mu\nu} = i\hbar(G_{LR})_{\mu\nu}\sqrt{v_\mu v_\nu}, \quad (14)$$

$$r_{\mu\nu} = -\delta_{\mu\nu} + i\hbar(G_L)_{\mu\nu}\sqrt{v_\mu v_\nu}, \quad (15)$$

$$t'_{\mu\nu} = i\hbar(G_{RL})_{\mu\nu}\sqrt{v_\mu v_\nu}, \quad (16)$$

$$r'_{\mu\nu} = -\delta_{\mu\nu} + i\hbar(G_R)_{\mu\nu}\sqrt{v_\mu v_\nu}, \quad (17)$$

where v_μ is the group velocity associated to the electronic component of the state $|\mu\rangle = |k; n_\alpha, n_\beta, \dots\rangle$

$$v_\mu = -\frac{2\beta_L}{\hbar} \sin(k) . \quad (18)$$

$t_{\mu\nu}$ and $r_{\mu\nu}$ are respectively the transmission and reflection amplitude for states incoming from the left-hand side lead, while $t'_{\mu\nu}$ and $r'_{\mu\nu}$ are the same quantities but for states incoming from the right-hand side lead.

Finally the current can be extracted from the Landauer formula [15]

$$I = \frac{2e}{h} \int \sum_{\mu\nu} [|t_{\mu\nu}|^2 F_L(E) - |t'_{\mu\nu}|^2 F_R(E)] dE , \quad (19)$$

where $F_L(E)$ and $F_R(E)$ are the Fermi distributions respectively for left- and right-hand side lead. Note that in the case of time-reversal symmetry $t_{\mu\nu} = t'_{\mu\nu}$ and the current becomes

$$I = \frac{2e}{h} \int \sum_{\mu\nu} |t_{\mu\nu}(E)|^2 [F_L(E) - F_R(E)] dE . \quad (20)$$

D. Pauli principle

For elastic transport different scattering channels do not compete for the same final state, since the scattering wave-functions extend from one lead to the other. This is also formally true for our fictitious system. However when one considers the electronic part of the fictitious system, the situation appears rather different. Consider for example the scattering process in which $|k; n_\alpha, n_\beta, \dots\rangle$ is transmitted into the same state $|k; n_\alpha, n_\beta, \dots\rangle$, and the one in which it is the state $|k'; m_\alpha, m_\beta, \dots\rangle$ to be transmitted into $|k; n_\alpha, n_\beta, \dots\rangle$. In the first process the phononic configurations of the initial and final states are identical and therefore the scattering is elastic. In contrast the second process involves a change in phononic configuration, which means that energy has been exchanged between the electronic and the phononic sub-systems. This is an inelastic scattering event.

The crucial point is that these two processes lead to the same final electronic state $|k\rangle$, the first through elastic and the second through inelastic scattering. These two scattering events do not share the same scattering wave-function and therefore compete for the same electronic states. Therefore in this case the Pauli exclusion principle should be taken explicitly into consideration when evaluating the current.

We then use the procedure introduced by Emberly and Kirczenow [16], which evaluates self-consistently the non-equilibrium electron distributions resulting from the Pauli principle. We define $(f_{+,el}^{\alpha\alpha})^R(E')$ as the electronic distribution of the right-hand side lead resulting from electrons transmitted elastically from left to right at an energy E' . As a matter of notation we label with “+”

(“−”) scattering processes involving electron transmission (reflection), “R” (“L”) indicates that the distribution is for the right-hand side (left-hand side) lead, and “el” that the scattering process is elastic. Finally the indexes α label the associated states $|\alpha\rangle = |k; n_\alpha, n_\beta, \dots\rangle$ describing the process. Similarly $(f_{+,in}^{\alpha\alpha'})^R(E')$ is the elec-

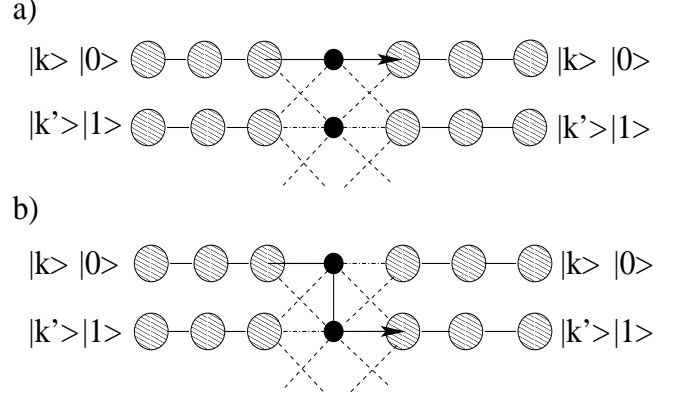


FIG. 4: Scattering events of the fictitious system, contributing to the various electronic distributions. (a) elastic scattering of the state $|k; 0\rangle = |k\rangle|0\rangle$, contributing to the distribution $(f_{+,el}^{\alpha\alpha})^R(E')$. (b) inelastic scattering of the state $|k; 0\rangle = |k\rangle|0\rangle$ into the state $|k'; 1\rangle = |k'\rangle|1\rangle$ contributing to the distribution $(f_{+,in}^{\alpha\alpha'})^R(E')$.

tronic distributions in the right-hand side lead given by electrons incoming from the left-hand side lead and inelastically transmitted through the molecule (Fig 4). In this case E' is the energy of the final electronic state and the scattering is between the states $|\alpha\rangle = |k; n_\alpha, n_\beta, \dots\rangle$ and $|\alpha'\rangle = |k'; m_\alpha, m_\beta, \dots\rangle$.

If one neglects Pauli's principle these quantities are simply related to the Fermi distributions of the lead containing the incoming electrons

$$(f_{+,el}^{\alpha\alpha})^R(E') = F_L(E') T^{\alpha\alpha}(E', E') , \quad (21)$$

$$(f_{+,in}^{\alpha\alpha'})^R(E') = F_L(E) T^{\alpha\alpha'}(E, E') , \quad (22)$$

where we have introduced the transmission coefficients $T^{\alpha\beta}(E, E') = |t_{\alpha\beta}|^2$, which depend on both the initial E and final E' electronic energy. All the other distributions, for electrons approaching from the right-hand side lead, can be written in a completely analogous way [16].

We now need to establish a procedure for evaluating the distributions f in such a way of accounting for Pauli exclusion principle. This is easily done by imposing that a generic distribution f is given by the combined probability of transmitting an electron with that of finding the final state empty. For instance the distribution of elastically transmitted electrons in the right-hand side lead

reads

$$(f_{+,el}^{\alpha\alpha'})^R(E') = F_L(E')c(E')T^{\alpha\alpha'}(E', E') \times [1 - \sum_{\alpha' \neq \alpha} (f_{+,in}^{\alpha\alpha'})^R(E') - \sum_{\alpha' \neq \alpha} (f_{-,in}^{\alpha\alpha'})^R(E')] . \quad (23)$$

This means that the distribution in the right-hand side lead of electrons elastically transmitted at an energy E' is proportional to the probability of transmitting an initially filled state in the left-hand side lead $F_L(E')T^{\alpha\alpha'}(E', E')$, and to the probability that the final state is not already occupied $[1 - \sum_{\alpha' \neq \alpha} (f_{+,in}^{\alpha\alpha'})^R(E') - \sum_{\alpha' \neq \alpha} (f_{-,in}^{\alpha\alpha'})^R(E')]$. This last probability is determined by two competing effects: inelastic transmission from the left-hand side lead $(f_{+,in}^{\alpha\alpha'})^R$, and inelastic reflection from the right-hand side lead $(f_{-,in}^{\alpha\alpha'})^R$.

Similar equations can be derived for all the other distributions in the right-hand side lead

$$(f_{+,in}^{\alpha\alpha'})^R(E') = F_L(E)c(E)T^{\alpha\alpha'}(E, E') \times [1 - (f_{+,el}^{\alpha\alpha'})^R(E') - (f_{-,el}^{\alpha\alpha'})^R(E') - \sum_{\beta \neq \alpha} (f_{+,in}^{\alpha\beta})^R(E') - \sum_{\alpha' \neq \alpha} (f_{-,in}^{\alpha\alpha'})^R(E')] , \quad (24)$$

$$(f_{-,el}^{\alpha\alpha'})^R(E') = F_R(E')d(E')R^{\alpha\alpha'}(E', E') \times [1 - \sum_{\alpha' \neq \alpha} (f_{+,in}^{\alpha\alpha'})^R(E') - \sum_{\alpha' \neq \alpha} (f_{-,in}^{\alpha\alpha'})^R(E')] , \quad (25)$$

$$(f_{-,in}^{\alpha\alpha'})^R(E') = F_R(E)d(E)R^{\alpha\alpha'}(E, E') \times [1 - (f_{+,el}^{\alpha\alpha'})^R(E') - (f_{-,el}^{\alpha\alpha'})^R(E') - \sum_{\beta \neq \alpha} (f_{-,in}^{\alpha\beta})^R(E') - \sum_{\alpha' \neq \alpha} (f_{+,in}^{\alpha\alpha'})^R(E)] , \quad (26)$$

where $(f_{+,in}^{\alpha\alpha'})^R(E')$, $(f_{-,el}^{\alpha\alpha'})^R(E')$ and $(f_{-,in}^{\alpha\alpha'})^R(E')$ are the distributions for electron undergoing respectively to inelastic transmission, elastic reflection and inelastic reflection, and we have introduced the reflection coefficient $R^{\alpha\beta}(E, E') = |r_{\alpha\beta}|^2$. Analogous expression for the left-hand side lead can be obtained by replacing $R \rightarrow L$, $T^{\alpha\beta} \rightarrow T^{\alpha\beta'}$ and $R^{\alpha\beta} \rightarrow R^{\alpha\beta'} = |r'_{\alpha\beta}|^2$ in the equations (23) through (26).

The normalization functions $c(E)$ and $d(E)$ are obtained by imposing charge conservation deep into the leads, which means that the sum of all the distributions f must be equal to the equilibrium Fermi distribution of the particular lead

$$F_L(E) = (f_{+,el}^{\alpha\alpha})^R(E) + (f_{-,el}^{\alpha\alpha})^L(E) + \sum_{\alpha'} (f_{+,in}^{\alpha\alpha'})^R(E') + \sum_{\alpha'} (f_{-,in}^{\alpha\alpha'})^L(E') , \quad (27)$$

$$F_R(E) = (f_{+,el}^{\alpha\alpha})^L(E) + (f_{-,el}^{\alpha\alpha})^R(E) + \sum_{\alpha'} (f_{+,in}^{\alpha\alpha'})^L(E') + \sum_{\alpha'} (f_{-,in}^{\alpha\alpha'})^R(E') . \quad (28)$$

The equations (27) and (28) together with those for the distributions (23), (24), (25) and (26) form a close set of equations, that can be solved for the f iteratively. These are evaluated numerically over a discrete energy mesh. Finally the current is obtained by a direct extension of the Landauer formula, which takes into account the self-consistent electron distributions

$$I = \frac{2e}{h} \int \left(\sum_{\alpha} \left[(f_{+,el}^{\alpha\alpha})^R(E) + \sum_{\alpha'} (f_{+,in}^{\alpha\alpha'})^R(E) \right] - \sum_{\alpha} \left[(f_{+,el}^{\alpha\alpha})^L(E) + \sum_{\alpha'} (f_{+,in}^{\alpha\alpha'})^L(E) \right] \right) dE . \quad (29)$$

III. RESULTS

We are now in the position of investigating inelastic transport in atomic scaled systems. In particular we will consider three material systems. The first is a simple diatomic molecule. This will be used as a test case for explaining some general concepts of inelastic transport and for providing details about the convergence. Then we will investigate the case of the H_2 molecule, for which experimental data are available [40]. Finally we will move our attention to the investigation of inelastic scattering in molecular spin-valves made from half-metallic leads. In all the calculations we consider temperatures considerably lower than the energy of the lowest of the phonon modes. This means that $|k; 0, 0, \dots\rangle$ is the only occupied incoming channel and that there cannot be a net phonon absorption.

A. Fixing the phonon cutoff

The first system that we consider is a diatomic molecule sandwiched between two identical mono-dimensional leads. These are described by a single orbital nearest neighbor tight-binding model with on-site energy $\epsilon_L = \epsilon_R = -10$ eV and hopping parameter $\beta_L = \beta_R = 2$ eV (the total bandwidth is 8 eV). The Fermi level of the leads is taken at $E_F = -10$ eV, which corresponds to half-filling. The tight-binding parameters of the diatomic molecule are taken from reference [16] and are $\epsilon_M = -10$ eV, $w^0 = 0.15$ eV, $t_{ij} = 0.2$ eV, $\alpha_{ij} = 6.1$ eV/Å. The masses of the atoms in the molecule are 13 a.m.u. (each site corresponds to a C-H group) and the spring constants are $K_{\text{lead-M}} = 180$ eV/Å², and $K_M = 90$ eV/Å², where the first is the one between the leads and the molecule and the second is the intra-molecular one.

These parameters lead to two longitudinal phonons (the only ones considered here) of energies $\hbar\omega_1 = 0.24$ eV and $\hbar\omega_2 = 0.33$ eV. A schematic diagram of the energy level alignment is presented in figure 5. The main goal of this section is to discuss how the energy mesh and the number of phonon states included in the calculation affect the results.

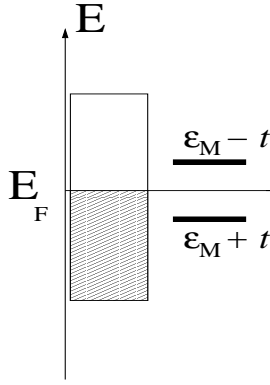


FIG. 5: Schematic representation of the energy level lineup of the diatomic molecule discussed in this section. The solid box represents the density of states of the mono-atomic leads, the solid horizontal lines denote the position of the bonding and antibonding states of the free molecule and the thin horizontal line is the position of the Fermi level E_F .

The general strategy for testing the convergence of the calculation is as follows. First one investigate how the transmission coefficient changes with the number of phonon states N_{ph} included in the calculation. This is done with a reasonably fine energy mesh in order to have a good energy resolution. Then, once N_{ph} is fixed, the energy meshed is varied and the convergence of the current is controlled. Note that the energy mesh and the cutoff over the number of phonon states have two deeply different physical meanings. The energy mesh merely controls how accurate is the energy resolution, and typically a resolution of the order of 1 meV is sufficient. In contrast the number of phonon states essentially establishes the degree of accuracy in describing multiple phonon scattering.

In figure 6 we show the total transmission coefficient (elastic plus inelastic) at zero bias as a function of energy for different numbers of phonon states $|n_1, n_2\rangle$ included in the calculation. It is clear that as N_{ph} increases the transmission coefficient becomes more broadly distributed in energy and the resonances are largely smeared out. When no phonons are present $T(E)$ has only two sharp resonances, located at the bonding and anti-bonding energies of the molecule, with a broadening proportional to the electronic coupling with the leads. The inclusion of phonon absorption/emission opens new scattering channel where phonon-assisted hopping to the molecular level becomes possible. This broadens the spectral range of $T(E)$ and shifts the transmission peaks. In particular the resonance at the bonding state shifts almost rigidly of about 0.15 eV towards lower energies, while that at the antibonding level gets substantially smeared.

This behavior is somehow expected since in our working conditions of low temperature electrons cannot be transmitted with a net energy gain (no net phonon absorption is allowed). Thus most of the spectral modifications due to electron-phonon scattering occur above

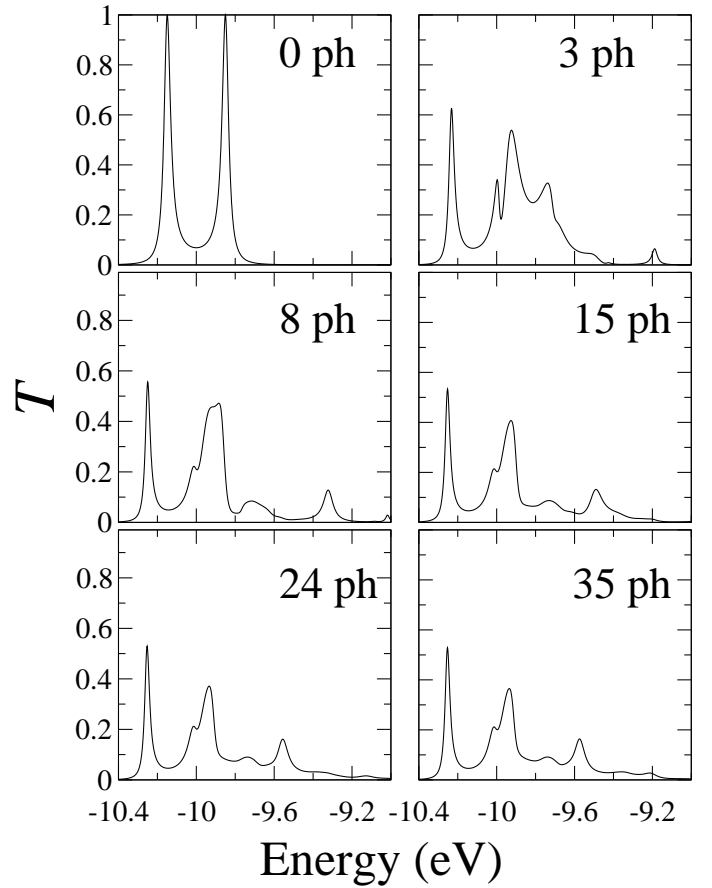


FIG. 6: Total transmission coefficient (elastic plus inelastic) as a function of the energy obtained for an increasing number of phonon states N_{ph} . The convergence is obtained for 24 states (solid line), that is a maximum occupation of $n_{\alpha}=5$ for each phonon mode.

the Fermi level. If we now focus our attention on the transmission coefficient for $N_{\text{ph}}=24$ (the higher occupation allowed is $n_{\alpha}=5$ for both the phonon modes) we can associate the first peak at about -10.25 eV with resonant elastic transport through the bonding state, the second just below -10.0 eV with phonon-assisted resonant transport through the bonding state via the first phonon mode ($\hbar\omega_1=0.24$ eV), the third at about -9.92 eV with phonon-assisted resonant transport through the bonding state via the second phonon mode ($\hbar\omega_2=0.33$ eV), and so on. Note that peaks in the transmission coefficient appearing at rather high energies are the result of resonant transport through either the bonding or the antibonding level via multiple phonon emission.

Note also that upon increasing the number of phonon states $T(E)$ is only weakly affected for low energies, but changes drastically at high energies. This is because new scattering paths involving multiple phonon emission become available. However these high order multiple scattering events are increasingly improbable and one expects $T(E)$ to saturate for N_{ph} large enough. As a measure of the convergence of T with the number of phonon modes we evaluate the mean deviation Δ_{mn} between the trans-

mission coefficients T_m and T_n calculated respectively for $N_{\text{ph}}=m$ and $N_{\text{ph}}=n$

$$\Delta_{mn} = \frac{1}{M} \sum_i^M |T_m(E_i) - T_n(E_i)|, \quad (30)$$

with the sum running over the energy mesh points. The values of Δ_{mn} for the transmission coefficients of figure 6 are respectively $\Delta_{0,3}=0.0242$, $\Delta_{3,8}=0.0121$, $\Delta_{8,15}=0.0065$, $\Delta_{15,24}=0.0030$ and $\Delta_{24,35}=0.0012$. A value of $\Delta \sim 0.0015$ is usually considered as a good level of convergence.

The convergence of the transmission coefficients clearly guarantees the convergence of all the quantities related to them. Therefore after having determined N_{ph} we can then calculate the current using equation (29). In figure 7 we show the elastic and inelastic contributions to the I - V characteristic and the total current (elastic plus inelastic) as a function of N_{ph} for different biases. A simple rule of thumbs for understanding the features of the I - V curve is that most of the current originates from the total transmission coefficient in an energy window comprised between $E_F + V/2$ and $E_F - V/2$. Note that this is only approximately valid when electron-phonon scattering is present. In fact the self-consistent electron distributions f can provide some non-vanishing contributions to the current coming from transmission coefficients outside this energy window.

First consider the case in which $N_{\text{ph}}=0$, i.e. the purely elastic case. The I - V has only the elastic component and shows three different slopes, corresponding to three different resistances. For bias below 0.2 Volt the transmission is small, since no molecular state is comprised in the bias window. Then for voltages between 0.2 and 0.4 Volt, both the bonding and the antibonding states of the molecule appear in the bias window, producing a large increase of the current. Finally for higher biases the current saturates since no new molecular states are available for transport.

The main effects of switching on the electron-phonon interaction $N_{\text{ph}} \neq 0$ is that the inelastic current starts to participate to the conductance. This is almost zero for biases up to about 0.2 Volt, which is roughly the energy of the first phonon mode, and then increase almost linearly with bias. This opening of phonon-assisted transport channels appears in the I - V curve as a peak in the derivative of the differential conductance, a property which is used for detecting molecular vibrations from transport measurements [39, 40, 41]. Note that phonon emission for biases smaller than the energy of the first phonon mode is certainly possible. However this process contributes little to the current, since the final state has high probability to be filled. Note also that the elastic current for small biases increases with respect to the purely elastic case. This is due to the contribution of multiple scattering, which effectively increases the value of the transmission coefficient around E_F (see figure 6). The relative portions of elastic and inelastic current de-

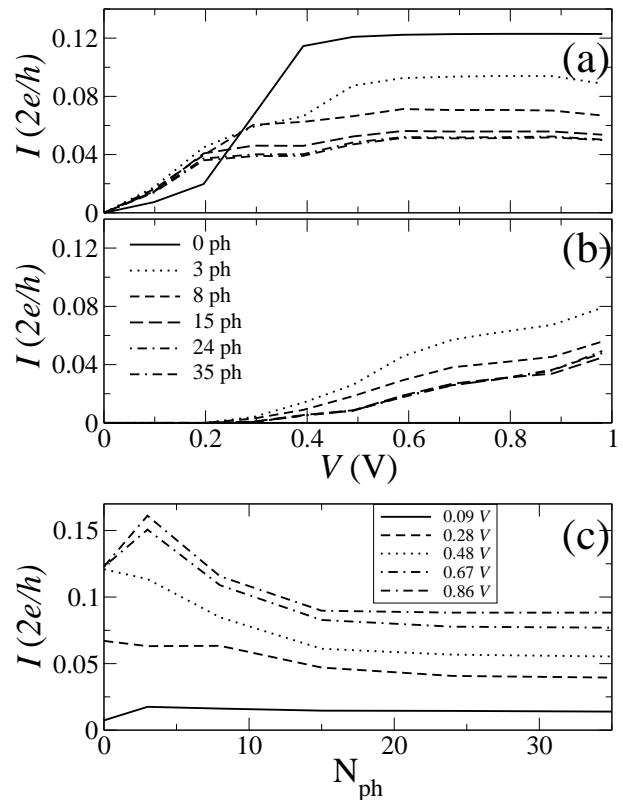


FIG. 7: a) Elastic current for different phonon cutoffs. b) Inelastic current for different phonon cutoffs. c) Total current (elastic+inelastic) as a function of number of phonons. Each line represents different voltages. At $V=0$ the total current is always 0.

pend on the details of the Hamiltonian, however our analysis demonstrate that a considerable number of phonon states must be included in the calculations for saturating the current.

Figure 8 shows the same currents of figure 7, this time obtained without imposing the Pauli exclusion principle through the distributions f . The most evident difference is that now the inelastic current does not vanish for $V < 0.2$ Volt, i.e. for biases smaller than the energy of the first phonon mode. This happens since the occupation of the final state is not considered, thus transmission to final energies below $E_F - V/2$ (the chemical potential of the right-hand side lead) is possible. As a consequence the elastic current in the same bias region is reduced with respect to the previous case. Finally note that the currents calculated either imposing or not imposing the Pauli principle are similar for large biases, where the vast majority of the incoming states is filled, and the final states are empty.

B. Transport through H_2 molecules

Platinum point contacts sandwiching H_2 molecules represent the ideal system, where to investigate the effects of electron-phonon interaction on the electron trans-

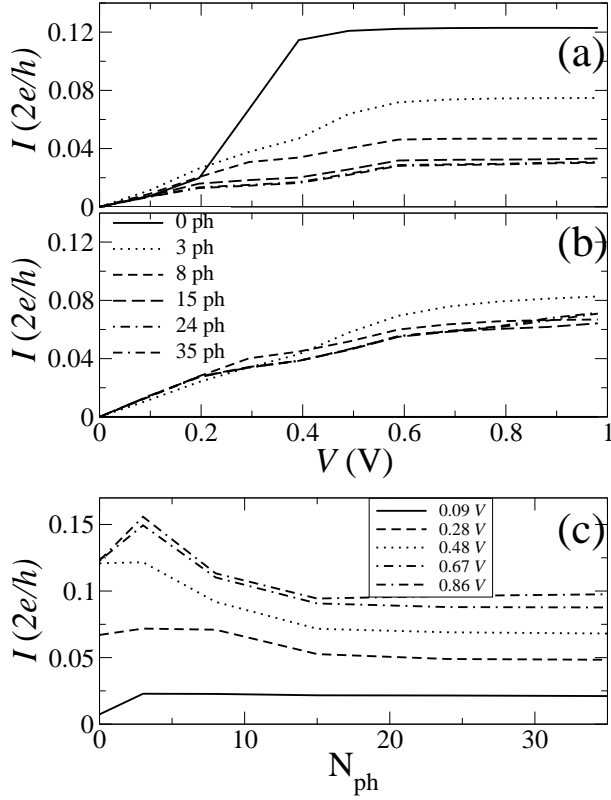


FIG. 8: a) Elastic current for different phonon cutoffs, calculated without considering the exclusion principle. b) Inelastic current for different phonon cutoffs, calculated without considering the exclusion principle. c) Total current (elastic+inelastic) calculated without considering the exclusion principle (elastic+inelastic) as a function of the number of phonons. Each line represents different voltages. At $V=0$ the total current is always 0.

port. These contacts in fact are stable for long times, enabling the measurement of low bias I - V characteristics under different stretching conditions [40]. The most important aspect of the current/voltage curves is a rather sharp drop of the differential conductance $G_R(V) = \frac{dI}{dV}$ from a value of approximately $G_0 = 2e^2/h$ for voltages close to 63 mV. This corresponds to a peak in the derivative of G_R , $\frac{dG_R}{dV}$, and it is attributed to the onset of electron-phonon scattering to the lowest phonon mode available in the junction [40].

Despite the initial controversy [42] recent *ab initio* calculations [43, 44] have convincingly proved that the transport in this system occurs through the antibonding state of the H_2 molecule in the so called “bridge” configuration, i.e. with the molecular bond lying parallel to the transport direction. The antibonding state provides a high transmission channel and the differential conductance is about $0.9 G_0$. Moreover *ab initio* calculations have also suggested that a transversal vibrational mode of the H_2 molecule is responsible for the differential conductance drop at ~ 60 meV [44]. This last identification, although supported by the blue-shift of the differential conductance drop upon stretching, however is more dif-

ficult to establish since the local arrangement of the Pt atoms at the tip is unknown (it is likely that the H_2 molecule bridges the Pt contacts in a zig-zag geometry [43]).

In an attempt of understanding the main mechanism responsible for the drop of $G_R(V)$ and to provide a further test to our scheme, we model a Pt- H_2 -Pt point contact as two semi-infinite monoatomic current/voltage leads sandwiching a H_2 molecule. The leads are at half-filling with on-site energy $\epsilon_0=0$ eV and hopping parameter $\gamma=5.0$ eV. This guarantees a rather large (20 eV) bandwidth. The tight-binding parameters for the H_2 molecule are chosen in such a way of aligning the antibonding state at the Fermi level and to give a conductance close to $0.97 G_0$ for zero bias [40]. We consider as relevant phonon modes only longitudinal modes and we tune the electron-phonon coupling in such a way of reproducing the experimental drop of the differential conductance. Note that at this level of approximation the choice of using either transverse or longitudinal modes is somehow immaterial.

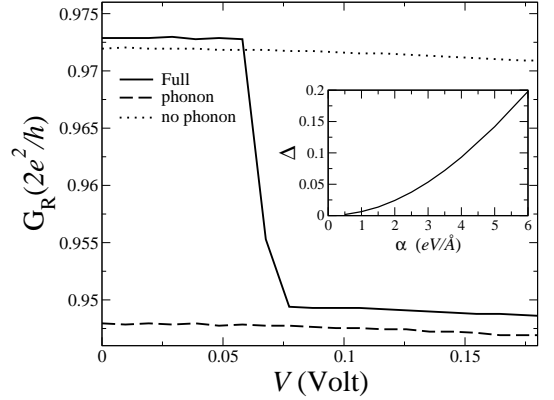


FIG. 9: Differential conductance for the H_2 molecule sandwiched between Pt leads. The solid line is for the full calculation where both the Pauli principle and electron-phonon interaction are included, the line labeled with “phonons” is for a the calculation done without considering the Pauli principle and the line labeled with “no phonons” is for purely elastic transport. In the inset the drop of the differential conductance as a function of the electron-phonon coupling α . The relative drop Δ is defined as the ratio between the differential conductance at V just above the first phonon energy ($V=63$ mV) and that at zero bias $\Delta = [G_R(V) - G_R(0)]/G_R(0)$.

Figure 9 summarizes the main result of our calculations. Clearly, when both electron-phonon interaction and Pauli principle are considered the differential conductance has a drop for voltages around 60 mV, which corresponds to the energy of the first longitudinal phonon mode at 63 meV (oscillation of the center of mass of H_2). This drop of G_R is due to the enhancement of inelastic back-scattering, which reduces the transmission of the elastic channel resonant at the antibonding state and it has the net effect of suppressing the current. In fact a careful analysis of the electron distributions f has revealed a peak in $f_{-,in}^L$ for energies corresponding to the emission of the first longitudinal phonon. This emis-

sion, leading to the enhanced inelastic back-scattering is Pauli suppressed for biases V such that $eV < \hbar\omega_1$, but it becomes possible as soon as the bias window is large enough to allow the phonon emission. Furthermore, within our simplified model we do not expect any additional differential conductance drop for small bias, since the next longitudinal phonon mode has a rather high energy (~ 430 meV).

Note that such a drop of G_R for $eV \sim \hbar\omega_1$ cannot be described unless both electron-phonon coupling and Pauli principle are considered. On the one hand, when the Pauli principle is neglected the inelastic back-scattering is always present and contribute to the current, with the net result that no conductance drop is found. In this case the conductance has a value similar to that obtained for $V > 63$ mV. On the other hand, if electron-phonon interaction is set to zero, no drop can be found since inelastic back-scattering is not included. The conductance now is similar to that calculated for $V < 63$ mV and almost independent from the bias.

Importantly the magnitude of the differential conductance drop depends on the strength of the electron-phonon coupling, and it grows as the coupling is enhanced. Such a behavior is demonstrated in the inset of figure where $[G_R(V) - G_R(0)]/G_R(0)$ is plotted as a function of the coupling α . Interestingly we found that $\Delta \propto \alpha^2$. Since the relevant longitudinal phonon mode is that of the center of mass of H_2 oscillating between the two Pt contacts, the only α determining the transport is that of the Pt-H bond. This is mainly an $ss\sigma$ bond [43], which roughly scales as $1/d^2$ with the separation d between Pt and H [45]. Such a scaling leads to $\Delta \propto 1/d^6$, and therefore we predict for longitudinal modes a very drastic dependence of the differential conductance drop as a function of the point contacts separation.

C. Molecular Spin-valves

Finally we investigate the effects of inelastic electron-phonon scattering on the transport properties and the GMR of a model spin-valve formed by half-metal current/voltage probes sandwiching an organic molecule. In particular we consider a $M_{\beta'}$ half-metal [27], in which the Fermi level cuts through the minority band (see figure 10). In our model calculation this is obtained by a linear chain of hydrogenic atoms whose on-site energies are spin-split. In particular we consider $\epsilon^\uparrow = -14$ eV for the majority (\uparrow) and $\epsilon^\downarrow = -6$ eV for the minority (\downarrow) spin bands. For both the spin-bands the hopping parameters are $\beta_L = \beta_R = -2$ eV, which give a bandwidth and an exchange of 8 eV. With this choice of parameters the majority upper band-edge coincide with the lower minority band-edge at $E = -10$ eV.

The molecules are linear chains of various lengths (from one to three atoms) made by atoms of mass 13 a.m.u. (C-H groups) and characterized by the hopping integral $t_{ij} = 0.2$ eV. The on-site energy of the molecule

is always close to the position of the Fermi level giving resonant transport through the molecular states. We have then investigated two possible situations. In the first one (see figure 10a) $\epsilon_M = -8.2$ eV and the Fermi level $E_F = -8.0$ eV is well within the minority band. In the second one $E_F = \epsilon_M = -9.7$ eV is close to the lower minority band edge (figure 10b). The hopping parameters between the molecule and the leads and the electron-phonon couplings are the same as reference [16], i.e. $w^0 = 0.15$ eV, $\alpha = 6.1$ eV/Å, $K_{\text{lead-M}} = 180$ eV/Å² and $K_M = 90$ eV/Å². This leads to phonon modes with the following energies: i) one atom chain, $\hbar\omega_1 = 0.34$ eV; ii) two-atom chain $\hbar\omega_1 = 0.24$ eV, $\hbar\omega_2 = 0.33$ eV; iii) three-atom chain $\hbar\omega_1 = 0.17$ eV, $\hbar\omega_2 = 0.30$ eV and $\hbar\omega_3 = 0.34$ eV.

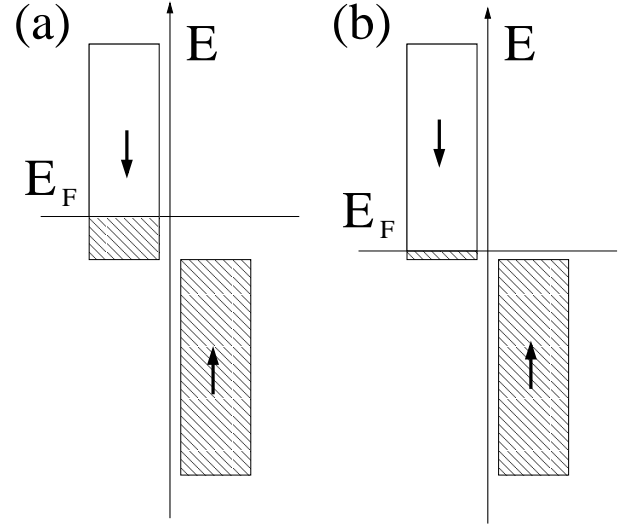


FIG. 10: Schematic representation of density of states for the model $M_{\beta'}$ half-metal and the two configurations studied: a) Fermi level well within the minority band, b) Fermi level close to the minority lower band-edge.

In investigating the spin-transport we consider the two spin fluids approximation where spin-flip scattering is neglected and the two spin sub-bands conduct in parallel. This is a good approximation for C-based organic molecules since both spin-orbit and hyperfine interactions are weak. The GMR is then defined as usual as

$$MR = \frac{I_P - I_{AP}}{I_P + I_{AP}}, \quad (31)$$

where I_P is the current of the spin-valve when the magnetization vectors of the two leads are parallel to each other and I_{AP} that for the antiparallel alignment. Within the two spin fluid model these read $I_P = I^{\uparrow\uparrow} + I^{\downarrow\downarrow}$ and $I_{AP} = I^{\uparrow\downarrow} + I^{\downarrow\uparrow}$, with $I^{\alpha\beta}$ the spin current and the index α (β) indicating the spin direction in the left-hand side (right-hand side) lead. Thus for instance $I^{\uparrow\downarrow}$ is the spin current for the antiparallel configuration where electrons propagate in the majority band in the left-hand side lead and in the minority in the right-hand side lead.

Let us consider first the case when $\epsilon_M = -8.2$ eV and $E_F = -8.0$ eV. In this situation the current is not negligible only for the minority spins in the parallel configuration $I^{\downarrow\downarrow}$ at least for biases lower than 3.6 Volt, after which also $I^{\uparrow\downarrow}$ gives contributions. In fact the particular density of states of our model half-metal and the relatively large Fermi level, result in the fact that for all the other configurations the density of states (DOS) of one of the two leads vanishes within the relevant bias window. The current is therefore completely suppressed by the lack of available states in the leads, and the GMR is always 1. Note that in principle multiple phonon emission might result in finite current also for other configurations, however this is always entirely suppressed by the Pauli exclusion principle.

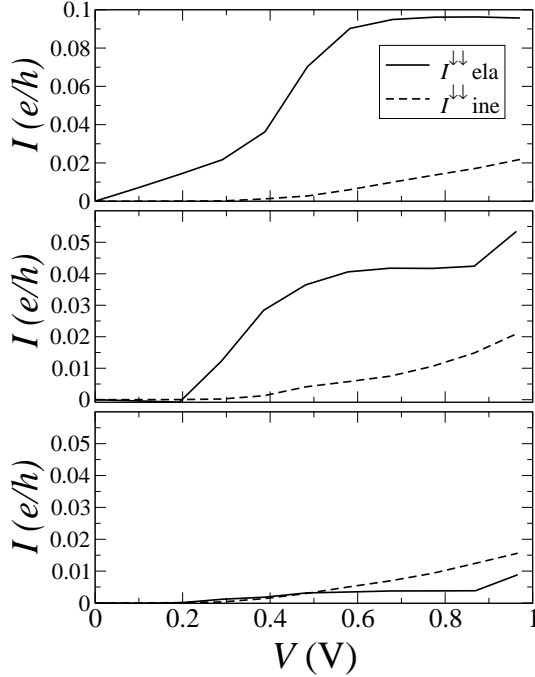


FIG. 11: I - V characteristic for the model spin-valve with $E_F = \epsilon_M = -8.2$ eV described in the text. The molecules are formed respectively from one atom (upper panel), two atoms (middle panel) and three atoms (lower panel). The only non-negligible contribution to the current is from the minority electrons in the parallel configuration $I^{\downarrow\downarrow}$.

The calculated I - V for the parallel case (up to 1 Volt) is presented in figure 11 for the three atomic chains investigated. The most notable feature is the drastic suppression of the elastic current as the chain length increases, and the fact that the inelastic component is only weakly affected. This is somehow expected since as the molecules becomes longer the direct tunneling probability decays and the current is dominated by the inelastic component. Interestingly, for this choice of parameters, reproducing $(CH)_n$ molecules, the inelastic current dominates already for rather short lengths ($n=3$).

The second case, when $E_F = \epsilon_M = -9.7$ eV is somehow different, since the Fermi level cuts much closer to

the minority lower band-edge. In this situation the half-metal DOS suppresses the current only at low bias and one expects transport in the antiparallel configuration, due to the $I^{\uparrow\downarrow}$ channel for biases as small as 0.6 eV. In fact at such biases finite DOS appears in the bias window for both the leads. This does not happen for the $I^{\uparrow\uparrow}$ and $I^{\downarrow\uparrow}$ contributions, which vanish at all biases. Therefore one has $I_P = I^{\downarrow\downarrow}$ and $I_{AP} = I^{\uparrow\downarrow}$ and the GMR is in general dependent on the bias.

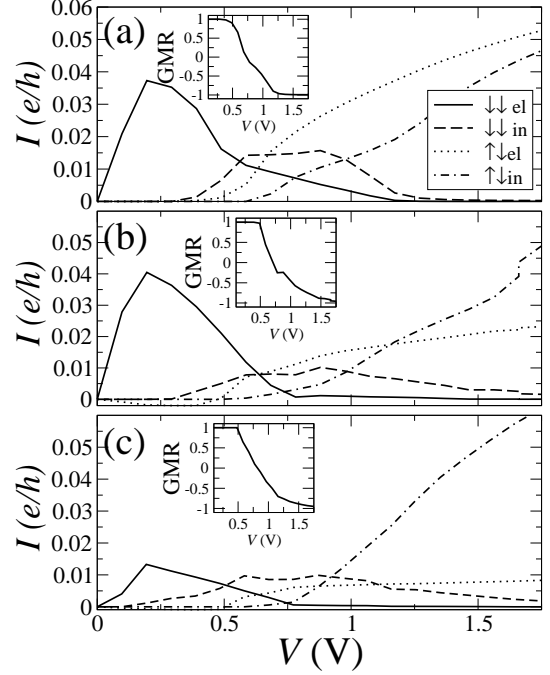


FIG. 12: I - V curves for the parallel and antiparallel configurations of a half-metal molecular spin-valve made from atomic chains containing (a) one, (b) two and (c) three atoms. In this case $E_F = \epsilon_M = -9.7$ eV, $I_P = I^{\downarrow\downarrow}$ and $I_{AP} = I^{\uparrow\downarrow}$. In the insets the corresponding GMR as a function of bias.

Figure 12 shows the I - V curves for both the parallel and antiparallel configurations of the spin-valve and the corresponding GMR, for molecules made respectively from one, two and three atoms. Let us consider first $I_P = I^{\downarrow\downarrow}$. The elastic component of the current dominates for voltages up to approximately 1.5 Volt, after which it gets completely suppressed. This suppression originates from the fact that the “effective” bias window (where both the leads have finite DOS) remains constant for $V > 0.6$ Volt, but it moves increasingly far from the energy levels of the molecular states. This drastically reduces the elastic transmission coefficient with a strong decrease of the current. The same effects somehow occurs for the inelastic component of the current although phonon emission allows transmission over a much wider energy window. This makes the inelastic component dominating for $V > 1$ Volt, regardless of the chain length.

In contrast in the antiparallel configuration no current can flow until the bias is large enough that the DOS of

the two leads overlap for some energies. This happens for $V \sim 0.5$ Volt for the elastic component and $V \sim 1.0$ Volt for the inelastic one. In this case we do not expect a decrease in the current for increasing bias, since the bias window is not cut by any band edge. As in the previous case the inelastic component becomes progressively more dominant as the chains gets longer and it is expected to dominate completely for very long chains. The resulting GMR is strongly bias dependent. In particular, for the present choice of parameters, it changes sign from positive at small bias to negative at high bias.

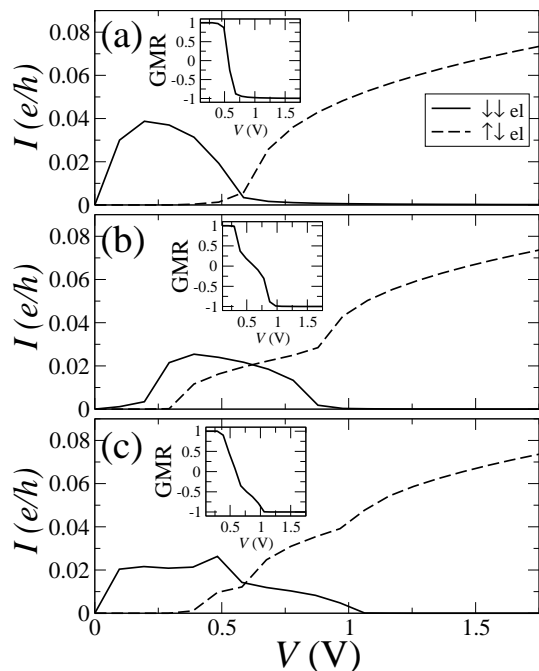


FIG. 13: Elastic I - V curves for the parallel and antiparallel configurations of a half-metal molecular spin-valve made from atomic chains containing (a) one, (b) two and (c) three atoms. In these calculations no electron-phonon interaction is considered. $E_F = \epsilon_M = -9.7$ eV and $I_P = I^{\downarrow\downarrow}$ and $I_{AP} = I^{\uparrow\downarrow}$. In the insets the corresponding GMR as a function of bias.

As a comparison in figure (13) we present results for the same systems obtained without electron-phonon interaction. In this case there is no substantial reduction of the elastic current as the molecular chain becomes longer, and the transport is always resonant through the molecular levels. However in absence of the inelastic component, the total current for the parallel alignment sharply decays for biases in excess of 1 Volt. As a consequence the GMR sharply changes from 1 to -1 as the bias increases.

Generally, inelastic scattering increases the spectral range (the energy region where the total transmission co-

efficient does not vanish) contributing to the current (see figure 6). In this case of half-metallic leads, the effect is to change the GMR as a function of bias. However if the leads are made from transition metals, then the effect of electron-phonon scattering is expected to be a change in the spin-polarization of the current [46]. This is connected to the increase of the spectral range of the transmission coefficient. A large spectral range means that a large portion of the ferromagnetic DOS contributes to the current. However in an ordinary transition metal the spin-polarization of the DOS is large at around E_F but decreases for both higher and lower energies. At higher energies this is due to the fact that there is little contribution from the d electrons for both spin directions, while at lower energy a large d -DOS is present for both spin directions. We therefore expect that electron-phonon interaction will produce a general suppression of the GMR.

IV. CONCLUSIONS

We have demonstrated the rôle of inelastic electron-phonon scattering on the transport properties of different nanoscale devices. This is treated using the multi-channel scheme introduced by Bonča and Trugman with the explicit inclusion of the Pauli exclusion principle. Such method allows us to map a scattering problem with inelastic effects, onto a fictitious problem where only elastic scattering events are present. We have then given a full description of the method, within our surface Green's function formalism, and described the criterion of convergence over the number and nature of phonon modes.

Two specific material systems have been investigated. The first are Pt point contacts sandwiching a H_2 molecule. In this case the differential conductance shows a sudden drop for a bias corresponding to the energy of the first H_2 longitudinal phonon mode, which we have explained as an enhancement of inelastic backscattering. Note that such a drop cannot be found unless the Pauli principle is considered.

Then we have investigated two types of spin-valves, obtained by contacting with half-metals a linear chain of CH groups. In this case the GMR depends on the specific alignment of the Fermi level with respect to the minority lower band-edge, and in general it is strongly bias dependent. The presence of electron-phonon scattering largely increases the current in the parallel state at high voltages and makes the change in GMR upon bias smoother with respect to the case where electron-phonons interaction is not considered.

[1] G. Prinz, Science **282**, 1660 (1998).

[2] S.A. Wolf et al., Science **294**, 1488 (2001).

[3] J.M. Daughton, J. Magn. Magn. Mat. **192**, 334 (1999).

[4] M.N. Baibich, J.M. Broto, A. Fert, F. Nguyen Van Dau,

- F. Petroff, P. Etienne, G. Creuzet, A. Friederich and J. Chazelas, Phys. Rev. Lett. **61**, 2472 (1988).
- [5] G. Binasch, P. Grünberg, F. Saurenbach and W. Zinn, Phys. Rev. B **39**, 4828 (1989).
- [6] I. Zutic, J. Fabian and S. Das Sarma, Rev. Mod. Phys. **76**, 323 (2004).
- [7] A.R. Rocha, V.M. Garcia Suarez, S.W. Bailey, C.J. Lambert, J. Ferrer and S. Sanvito, Nature Materials **4**, 335 (2005).
- [8] C. Joachim, J.K. Gimzewski and A. Aviram, Nature **408**, 541 (2000).
- [9] A. Aviram and M.A. Ratner, Chem. Phys. Lett. **29**, 277 (1974).
- [10] Z. H. Xiong, D. Wu, Z. Valy Vardeny and J. Shi, Nature (London) **427**, 821 (2004).
- [11] V. Dediu, M. Murgia, F.C. Matocota, C. Taliani, and S. Barbanera, Solid State Commun. **122**, 181(2002).
- [12] J. R. Petta, S. K. Slater and D. C. Ralph, Phys. Rev. Lett. **93**, 136601 (2004).
- [13] R. Pati, L. Sanapati, P. M. Ajayan and S.K. Nayak, Phys. Rev. B **68**, 100407(R) (2003).
- [14] E. G. Emberly and G. Kirczenow, Chem. Phys. **281**, 311-324 (2002).
- [15] S. Datta, *Electronic Transport in Mesoscopic Systems*, (Cambridge University Press, Cambridge, 1995)
- [16] E.G. Emberly and G. Kirczenow, Phys. Rev. B **61**, 5740 (2000).
- [17] H. Ness and A.J. Fisher, Phys. Rev. Lett. **83**, 452 (1999).
- [18] M. Galperin, M. Ratner and A. Nitzan, J. Chem. Phys. **121**, 11965 (2004).
- [19] M. Magoga and C. Joachim, Phys. Rev. B **57**, 1820 (1998).
- [20] P. Sautet and C. Joachim, Phys. Rev. B **38**, 12238 (1988).
- [21] N. Agrait et al, Phys. Rev. Lett **88**, 216803 (2002).
- [22] T. Frederiksen et al, Phys. Rev. Lett. **93**, 256601 (2004).
- [23] S.J. Xie, K.H. Ahn, D.L. Smith, A.R. Bishop and A. Saxena, Phys. Rev B **67**, 125202 (2003).
- [24] M.J. Montgomery, J. Hoekstra, T.N. Todorov and A.P. Sutton, J. Phys.: Cond. Matter **15**, 731 (2003).
- [25] S. Sanvito, C.J. Lambert, J.H. Jefferson and A.M. Bratkovsky, Phys. Rev. B **59**, 11936 (1999).
- [26] S. Sanvito, in *Handbook of Computational Nanotechnology*, American Scientific Publishers (Stevenson Ranch, California, 2005), also cond-mat/0503445.
- [27] J.M.D. Coey and S. Sanvito, J.Phys. D: Appl. Phys. **37**, 988 (2004).
- [28] A.R. Rocha and S. Sanvito, Phys. Rev. B **70**, 094406 (2004).
- [29] A.J. Heeger, S. Kivelson, J.R. Schrieffer and W.P. Su, Rev. Mod. Phys. **60**, 782 (1988).
- [30] W.P. Su, J.R. Schrieffer and A.J. Heeger, Phys. Rev. B **22**, 2099 (1980).
- [31] W.P. Su, J.R. Schrieffer and A.J. Heeger, Phys. Rev. Lett. **42**, 1698 (1979).
- [32] C.Kittel, *Introduction to Solid State Physics*, John Wiley and Sons (New York - 1953)
- [33] J. Bonča and S.A. Trugman, Phys. Rev. Lett. **75**, 2566 (1995).
- [34] K.Haule and J.Bonča, Phys. Rev. B **59**, 13087 (1999).
- [35] T. Frederiksen, M. Brandbyge, N. Lorente and A.-P. Jauho, Phys. Rev. Lett. **93**, 256601 (2004).
- [36] N. Jean and S. Sanvito, in preparation
- [37] M. Büttiker, Y. Imry, R. Landauer, and S. Pinhas, Phys. Rev. B **31**, 6207 (1985).
- [38] D.S. Fisher and P.A. Lee, Phys. Rev. B **23**, R6851 (1981).
- [39] B.S. Stime, M.A. Rezaei, and W. Ho, Science **280**, 1732 (1998).
- [40] R.H.M. Smit, Y. Noat, C. Untiedt, N.D. Lang, M. C. van Hemert, J.M. van Ruitenbeek, Nature (London) **419**, 906 (2002).
- [41] B.C. Stipe, M.A. Razaei and W. Ho, Phys. Rev. Lett. **81**, 1263 (1998) .
- [42] Y. García, J. J. Palacios, E. SanFabián, J. A. Vergés, A. J. Pérez-Jiménez, and E. Louis, Phys. Rev. B **69**, 041402(R) (2004).
- [43] V. M. Garcia Suárez, A. R. Rocha, S. W. Bailey, C. J. Lambert, S. Sanvito and J. Ferrer, Phys. Rev. B **72**, 045437 (2005).
- [44] D. Djukic, K.S. Thygesen, C. Untiedt, R.H.M. Smit, K.W. Jacobsen and J.M. van Ruitenbeek, Phys. Rev. B **71**, 161402(R) (2005).
- [45] W.A. Harrison, *Electronic Structure and Properties of Solids*, (Freeman, San Francisco, 1980)
- [46] I.I. Mazin, Phys. Rev. Lett. **83**, 1427 (1999).